and J. C. Irvin were greatly appreciated. The writers are indebted to M. Humpel for helpful suggestions and the actual construction of the frequency multiplier.

ERLING G. WESSEL†
Norwegian Defence Research Establ.
Dept. for Telecommunication
Postboks 25
Kjeller, Norway
ROBERT J. STRAIN‡
Standard Telecommunication Labs.
Harlow, Essex, England

† Formerly with University of Colorado, Boulder.
‡ Formerly with University of Illinois, Urbana.

TM and TE Mode Surface Waves on Grounded, Anisotropic, Inhomogeneous, Lossless, Dielectric Slabs*

J. H. Richmond has given the WKB solutions for the field distribution of surface waves on inhomogeneous, isotropic, plane layers.[1] It is the purpose of this letter to extend his work to include a simple anistropy in the dielectric constant by considering a diagonalized relative permittivity tensor with components $\epsilon_x(x)$, $\epsilon_y(x)$, and $\epsilon_z(x)$. The geometry is the same as before[1] except that a perfectly conducting plane is now positioned at $x=0$. For easy reference we have used the same notation as Richmond, except where specified otherwise. Compactness in notation has been achieved by expressing the integrations from 0 to x and by considering the x variations outside the slab to be $\exp\{-\alpha(x-a)\}$.

The TM solutions for the x variations of the field components are given by

$$H_y = \begin{cases} \exp\{-\alpha(x-a)\}, & \text{in region I,} \\ \dfrac{g(x)}{g(a)} \cdot \dfrac{\cos R(x)}{\cos R(a)}, & \text{in region II,} \end{cases} \quad (1)$$

$$E_z = \begin{cases} \dfrac{j\alpha}{\omega\epsilon_0} \cdot \exp\{-\alpha(x-\alpha)\}, & \text{in region I,} \\ \dfrac{j\alpha}{\omega\epsilon_0} \cdot \dfrac{g(a)}{g(x)} \cdot \dfrac{\sin R(x)}{\sin R(a)}, & \text{in region II,} \end{cases} \quad (2)$$

where

$$g(x) = \left[\frac{\epsilon_z(x)}{r(x)}\right]^{1/2}, \quad (3)$$

$$r(x) = \left[\frac{\epsilon_z(x)}{\epsilon_x(x)} \cdot (k^2\epsilon_x(x) - h^2)\right]^{1/2}, \quad (4)$$

and

$$R(x) = \int_0^x r(x)dx. \quad (5)$$

It is observed that H_y is normalized to unity at the air-slab interface. Also, we have considered the relative permeability of the slab to be unity.

The transcendental equation for the propagation constant h is given by

$$r(a) \tan R(a) = \alpha\epsilon_z(a). \quad (6)$$

Eq. (6), for a constant, scalar permittivity, reduces to (39) in a standard reference.[2]

The x variations for the TE modes are summarized as

$$E_y = \begin{cases} \exp\{-\alpha(x-a)\}, & \text{in region I,} \\ \left[\dfrac{q(a)}{q(x)}\right]^{1/2} \cdot \dfrac{\sin Q(x)}{\sin Q(a)}, & \text{in region II,} \end{cases} \quad (7)$$

$$H_z = \begin{cases} \dfrac{\alpha}{j\omega\mu_0} \exp\{-\alpha(x-a)\}, & \text{in region I,} \\ \dfrac{\alpha}{j\omega\mu_0} \cdot \left[\dfrac{q(x)}{q(a)}\right]^{1/2} \cdot \dfrac{\cos Q(x)}{\cos Q(a)}, & \text{in region II,} \end{cases} \quad (8)$$

where

$$q(x) = [k^2\epsilon_y(x) - h^2]^{1/2} \quad (9)$$

and

$$Q(x) = \int_0^x q(x)dx. \quad (10)$$

The determining equation for the propagation constant h is

$$q(a) \cot Q(a) = -\alpha, \quad (11)$$

which, for a constant, scalar permittivity, agrees with (46b) in a well-known text.[2]

It is to be noted that the solutions are valid only for slowly varying permittivities, or when

$$\left| \frac{r'(x)}{r^2(x)} - \frac{\epsilon_z'(x)}{r(x)\epsilon_z(x)} \right| \ll 2, \quad \text{TM}, \quad (12)$$

$$\left| \frac{q'(x)}{q^2(x)} \right| \ll 2, \quad \text{TE}, \quad (13)$$

where the prime denotes differentiation with respect to x. We find different restrictions on the TM and TE cases because the wave equations are different for the two cases, being given by

$$H_y'' - \frac{\epsilon_z'(x)}{\epsilon_z(x)} H_y' + \frac{\epsilon_z(x)}{\epsilon_x(x)} (k^2\epsilon_x(x) - h^2) H_y = 0, \quad \text{TM}, \quad (14)$$

and

$$E_y'' + (k^2\epsilon_y(x) - h^2)E_y = 0, \quad \text{TE}. \quad (15)$$

Expressions (12) and (13) can be verified by considering, in detail, standard WKB solutions of the Schroedinger equation.[3]

Conventionally,[1,4] we have neglected derivatives of $g(x)$ and $q(x)$ in finding E_z for the TM case and H_z for the TE case, respectively.

D. A. HOLMES
Westinghouse Electric Corp.
Research and Development Center
Pittsburgh 35, Pa.

* Received August 26, 1963.

[1] J. H. Richmond, "Propagation of surface waves on an inhomogeneous plane layer," IRE TRANS. ON MICROWAVE THEORY AND TECHNIQUES, vol. MTT-10, pp. 554–558; November, 1962.

[2] R. E. Collin, "Field Theory of Guided Waves," McGraw-Hill Book Company, Inc., New York, N. Y., ch. 11; 1960.

[3] L. I. Schiff, "Quantum Mechanics," McGraw-Hill Book Company, Inc., New York, N. Y., pp. 184–193; 1955.

[4] L. M. Brekhovskikh, "Waves in Layered Media," Academic Press, New York, N. Y., p. 196; 1960.

Application of Corner Mirrors for Ultramicrowave Interferometers*

The Michelson type and Fabry-Perot type interferometers are often used in the field of ultramicrowaves; the latter replace conventional cavity resonators in the millimeter and submillimeter wave range.[1]

The main problem connected with these devices is the design of suitable mirrors with low loss and adequate reflectivity. So far, planar or spherical mirrors are used.[2] Adjustment of these mirrors is critical and tedious; hence, the use of optical collimation methods is recommended.[3] These difficulties could be remarkably reduced by application of metallic mirrors in the form of rectangular prism corners, *i.e.*, so-called corner mirrors (see Fig. 1).

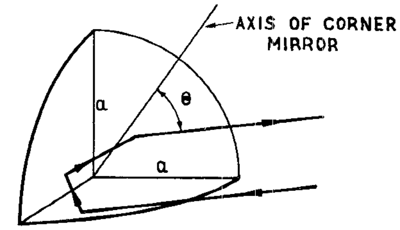

Fig. 1—Cubic corner mirror.

They take advantage of a very old principle of optics and have also been used sometimes in connection with radar techniques.[4] The adjustment of a corner mirror, which consists of three mutually perpendicular metallic plane mirrors, is in principle uncritical. For a correct design of a mirror, it is sufficient to secure the stable position of its peak. Then a beam of electromagnetic waves falling on a mirror at an angle of $\Theta < 35.26°$, after a triple reflection, will return antiparallelly to the falling beam. (For real mirrors having a finite ratio α/λ, a respectively smaller value of the angle Θ may be utilized.[1])

The interferometers utilizing corner mirrors could be designed in the form given in Figs. 2 and 3. The set in Fig. 2 differs from the conventional Michelson interferometer only by the type of the mirrors used, and, therefore, it does not require further discussion.

In the Fabry-Perot interferometer, one must secure suitable coupling with the cavity. For that purpose, one wall of the metallic corner should be half-transparent; a metallic perforated wall would be a good solution.[3] The Fabry-Perot interferometer with corner mirrors can be made in a number of variants (see Fig. 3). The set in Fig. 3(a) differs from that used in the past only by the type of mirrors used and additional

* Received August 16, 1963.

[1] W. Culshaw, "Resonators for millimeter and submillimeter wavelengths," IRE TRANS. ON MICROWAVE THEORY AND TECHNIQUES, vol. MTT-9, pp. 135–144; March, 1961.

[2] W. Culshaw, "Reflectors for microwave Fabry-Perot interferometer," IRE TRANS. ON MICROWAVE THEORY AND TECHNIQUES, vol. MTT-7, pp. 221–228; April 1959.

[3] W. Culshaw, "High resolution millimeter wave Fabry-Perot interferometer," IRE TRANS. ON MICROWAVE THEORY AND TECHNIQUES, vol. MTT-8, pp. 182–189; March, 1960.

[4] S. D. Robertson, "Targets for microwave radar navigation," *Bell Sys. Tech. J.*, vol. 26, pp. 852–869; October, 1947.

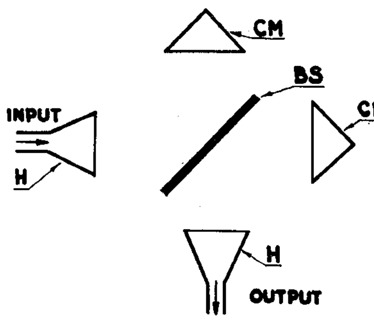

Fig. 2—Michelson interferometers with corner mirrors. H = horn, CM = corner mirror, BS = beam splitter.

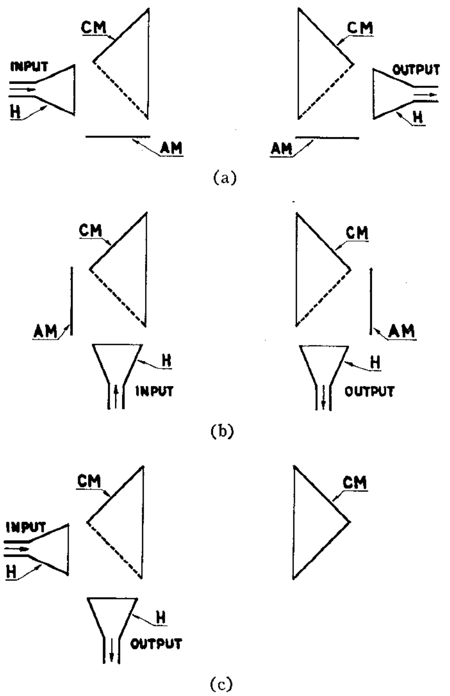

Fig. 3—Fabry-Perot interferometer variants with corner mirrors. H = horn, CM = corner mirror, AM = absorption mat.

absorption mats, without which the interferometer operation could be disturbed. The set in Fig. 3(b) has the horn axes situated parallel to one another. The variant in Fig. 3(c) is a further Fabry-Perot interferometer modification. Of course, in Figs. 3(b) and (c), a suitable setting of perforated plane mirror with respect to the horn is required.

A Fabry-Perot interferometer with corner mirrors possesses, besides previously mentioned insensitivity against misalignment, increased ruggedness—another valuable property. In this set there are no possibilities of the existence of unwanted multiple reflections in the space horn-mirror, since the corner mirror reflects onto the sides the waves falling on it from the back.

One could also apply in ultramicrowave interferometers, total internal reflection prisms, instead of metallic corner mirrors as was proposed with respect to lasers.[5] However, the available dielectric materials limit this scheme to rather lower Q cavities.

In the author's opinion, the application of corner mirrors for ultramicrowave interferometers instead of planar or spherical mirrors should simplify considerably the construction and improve the ruggedness of these instruments. It will also enable achievement of new constructional solutions.

The author would like to thank Prof. M. Suski and Prof. Z. Godziński for their useful and helpful discussions.

M. Kloza
Radio Dept.
Polytechnic Inst. Wroclaw
Wroclaw, Poland

[5] Z. Godziński, "Application of total internal reflection prism for gaseous lasers," Proc. IEEE (*Correspondence*), vol. 51, p. 361; February, 1963.

High-Order Varactor Multipliers*

The following correspondence is a report of the experimental results that have been obtained with a single-varactor-diode frequency multiplier. This circuit is a times sixteen (×16) single-stage varactor multiplier operating from 350 to 5600 Mc. The high efficiencies predicted theoretically for single-stage, high-order varactor multipliers are now being achieved with these practical circuits. They should have wide application in microwave systems where reliability and size are major considerations.

The ×16 varactor multiplier is part of a solid-state C-band local oscillator used in missile-borne radar transponders. It is driven by a crystal oscillator, a transistor amplifier and low-frequency multiplier circuits and utilizes a graded-junction silicon varactor in a series configuration packaged in a microminiature, ceramic, coaxial pill package. In addition to the varactor diode, which is loop coupled into a band-pass filter resonant at the output frequency, the circuit consists of an LC tuner resonant near the input frequency, a variable coaxial phase shifter and a low-pass filter with a cutoff frequency of approximately 1400 Mc. The VHF signal, supplied by the driver, is transmitted unattenuated through the tuner and low-pass filter and is converted into harmonics in the diode. The low-pass filter immediately adjacent to the diode reflects all harmonics above the fourth. The second, third and fourth harmonics flow through the low-pass filter and the phase shifter and are reflected back by the LC tuner. Low-loss idler paths are achieved by the phase shifter which controls the phases of the second through the fourth harmonics. The desired output frequency, the sixteenth harmonic in this instance, is selected by resonating the diode capacitance with the inductance formed by the coupling loop of the output band-pass filter. This filter is a miniature, two-section quarter-wavelength, coaxial cavity with a 3-db bandwidth of 20 Mc and an insertion loss of 2 db. Conversion efficiencies of 12 db—including the 2-db loss of the output filter—have been obtained with this high order varactor multiplier using diodes made by several different manufacturers. The diodes can be operated either with self bias or fixed dc bias.

* Received September 13, 1963.

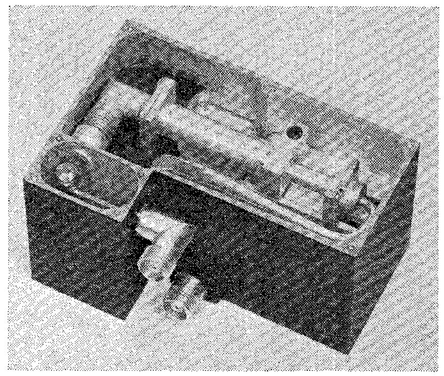

Fig. 1—×16 varactor multiplier in prototype package.

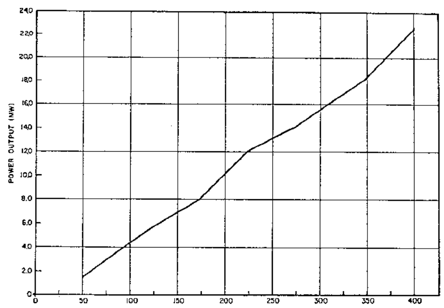

Fig. 2—Plot of typically obtained power output vs power input (f_0 = 5650 Mc).

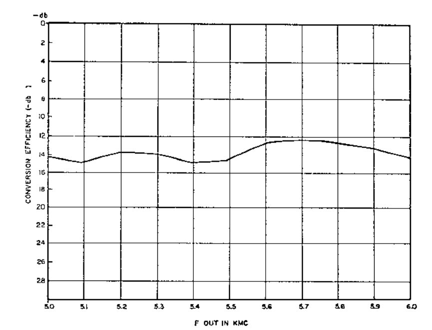

Fig. 3—×16 varactor multiplier tuned over a 1-kMc frequency range. Resulting increase in conversion loss is less than 3 db.

The ×16 varactor multiplier is shown in prototype package in Fig. 1. A plot of power output vs power input typically obtained is shown in Fig. 2. The multiplier has been tuned over a 1-kMc frequency range with a resultant increase in conversion loss of less than 3 db. This is shown in the curve of conversion efficiency plotted in Fig. 3. The instantaneous bandwidth of the multiplier is approximately 20 Mc over this 1-kMc tuning range. Both the instantaneous bandwidth and the tuning range are limited by characteristics of the output band-pass filter rather than by the varactor multiplier.

As part of a missile-borne system, the varactor multiplier has been subjected to severe environmental tests. It is capable of withstanding vibration of 20 g's in three planes, from 20–2000 cps (maximum double